

tutoring sessions, each 90 min, were given each day. Birds that produced soft (subsong) vocalizations during tutoring were banded and transferred to individual custom sound attenuating chambers where tutoring continued until a total of 60 days was reached. Eight birds were tutored with the forward phrase-pair ensemble, eight others received tutoring with the reversed phrase-pair regimen. Eleven birds were tutored with singly presented phrases.

Birds were sexed in the following summer either by microsatellite DNA analysis<sup>24</sup> or autopsy; five of the birds in the reversed phrase-order group and seven in the forward phrase-order group were confirmed to be males.

## Recording and analysis of vocalizations

The vocalizations of each bird were recorded using a small condenser microphone that was located in each sound-attenuating chamber. Beginning at approximately 30 days after tutoring, recordings were made frequently, with intervals not exceeding 9 days. These signals were digitized, displayed as spectrograms in real time and stored as computer files (Avisoft Recorder). Across renditions, the crystallized songs of birds often varied in length, with the last phrase sometimes not included. Spectrograms of crystallized songs that are displayed in this paper were chosen to show all of the phrase types of typical length found in these songs. Songs were scored with regard to whether adjacent phrases were placed in correct versus incorrect relative position; these values were then evaluated with respect to what would be expected by chance.

Received 2 July; accepted 31 August 2004; doi:10.1038/nature02992.

- Doupe, A. J. & Kuhl, P. K. Birds song and human speech: Common themes and mechanisms. *Annu. Rev. Neurosci.* **22**, 567–631 (1999).
- Konishi, M. The role of auditory feedback in the control of vocalization in the white-crowned sparrow. *Z. Tierpsychol.* **22**, 770–783 (1965).
- Thorpe, W. H. *Birdsong* (Cambridge Univ. Press, London, 1961).
- Konishi, M. *Perception and Experience* (Plenum, New York, 1978).
- Hultsch, H. & Todt, D. Discontinuous and incremental processes in the song learning of birds: Evidence for the primer effect. *J. Comp. Physiol.* **179**, 291–299 (1996).
- Marler, P. & Peters, S. Sparrows learn adult song and more from memory. *Science* **213**, 780–782 (1981).
- Soha, J. A. & Marler, P. Vocal syntax development in the white-crowned sparrow (*Zonotrichia leucophrys*). *J. Comp. Psychol.* **115**, 172–180 (2001).
- Marler, P. & Tamura, M. Song 'dialects' in three populations of white-crowned sparrows. *Condor* **64**, 363–399 (1962).
- Marler, P. & Tamura, M. Culturally transmitted patterns of vocal behavior in sparrows. *Science* **146**, 1483–1486 (1964).
- Marler, P. A comparative approach to vocal learning: Song development in white-crowned sparrows. *J. Comp. Physiol. Psychol.* **71**, 1–25 (1970).
- Tchernichovski, O., Mitra, P. P., Lints, T. & Nottebohm, E. Dynamics of the vocal imitation process: How a zebra finch learns its song. *Science* **291**, 2564–2569 (2001).
- Margoliash, D. Acoustic parameters underlying the responses of song-specific neurons in the white-crowned sparrow. *J. Neurosci.* **3**, 1039–1057 (1983).
- Margoliash, D. & Fortune, E. S. Temporal and harmonic combination sensitive neurons in the zebra finch's HVC. *J. Neurosci.* **12**, 4309–4326 (1992).
- Lewicki, M. S. & Arthur, B. J. Hierarchical organization of auditory temporal context sensitivity. *J. Neurosci.* **16**, 6987–6998 (1996).
- Lewicki, M. S. & Konishi, M. Mechanisms underlying the sensitivity of songbird forebrain neurons to temporal order. *Proc. Natl Acad. Sci. USA* **92**, 5582–5586 (1995).
- Lewicki, M. S. Intracellular characterization of song-specific neurons in the zebra finch auditory forebrain. *J. Neurosci.* **16**, 5854–5863 (1996).
- Mooney, R. Different subthreshold mechanisms underlie song selectivity in identified HVC neurons of the zebra finch. *J. Neurosci.* **20**, 5420–5436 (2000).
- Doupe, A. Song- and order-selective neurons in the songbird anterior forebrain and their emergence during vocal development. *J. Neurosci.* **17**, 1147–1167 (1997).
- Volman, S. F. Development of neural selectivity for birdsong during vocal learning. *J. Neurosci.* **13**, 4737–4747 (1993).
- Solis, M. M. & Doupe, A. Anterior forebrain neurons develop selectivity by an intermediate stage of song learning. *J. Neurosci.* **17**, 6447–6462 (1997).
- Bottjer, S. W., Miesner, E. A. & Arnold, A. P. Forebrain lesions disrupt development but not maintenance of song in passerine birds. *Science* **224**, 901–903 (1984).
- Aldridge, J. W. & Berridge, K. C. Coding of serial order by neostriatal neurons: a "natural action" approach to movement sequence. *J. Neurosci.* **7**, 2777–2787 (1998).
- Klein, D., Zatorre, R. J., Milner, B., Meyer, E. & Evans, A. C. Left putamen activation when speaking a second language: evidence from PET. *Neuroreport* **5**, 2295–2297 (1994).
- Griffiths, R., Double, M. C., Orr, K. & Dawson, R. J. G. A DNA test to sex most birds. *Mol. Ecol.* **7**, 1071–1075 (1998).

**Supplementary Information** accompanies the paper on [www.nature.com/nature](http://www.nature.com/nature).

**Acknowledgements** This work was supported by grants from the University of Utah and NIH. We thank T. Dance for technical assistance, E. Haskell for guidance in statistical analyses, J. Whittington for molecular sexing of birds and R. Dendukuri for writing computer programs used in analysis and presentation of data.

**Competing interests statement** The authors declare that they have no competing financial interests.

**Correspondence** and requests for materials should be addressed to G.R. (rose@bioscience.utah.edu).

## Early motor activity drives spindle bursts in the developing somatosensory cortex

Rustem Khazipov<sup>1,2,3\*</sup>, Anton Sirota<sup>2\*</sup>, Xavier Leinekugel<sup>1,2,4\*</sup>, Gregory L. Holmes<sup>3</sup>, Yehezkel Ben-Ari<sup>1</sup> & György Buzsáki<sup>2</sup>

<sup>1</sup>INMED, INSERM U29, Avenue de Luminy, B.P. 13, 13273 Marseille, France

<sup>2</sup>CMBN, Rutgers University, 197 University Avenue, Newark, New Jersey 07102, USA

<sup>3</sup>Section of Neurology, Neuroscience Center at Dartmouth, Dartmouth Medical School, One Medical Center Drive Lebanon, New Hampshire 03756, USA

<sup>4</sup>INSERM EMI 224, 105, Boulevard de l'Hôpital 75013 Paris, France

\* These authors contributed equally to this work

**Sensorimotor coordination emerges early in development. The maturation period is characterized by the establishment of somatotopic cortical maps<sup>1,2</sup>, the emergence of long-range cortical connections<sup>3</sup>, heightened experience-dependent plasticity<sup>4–7</sup> and spontaneous uncoordinated skeletal movement<sup>8,9</sup>. How these various processes cooperate to allow the somatosensory system to form a three-dimensional representation of the body is not known. In the visual system, interactions between spontaneous network patterns and afferent activity have been suggested to be vital for normal development<sup>10,11</sup>. Although several intrinsic cortical patterns of correlated neuronal activity have been described in developing somatosensory cortex *in vitro*<sup>12–14</sup>, the *in vivo* patterns in the critical developmental period and the influence of physiological sensory inputs on these patterns remain unknown. We report here that in the intact somatosensory cortex of the newborn rat *in vivo*, spatially confined spindle bursts represent the first and only organized network pattern. The localized spindles are selectively triggered in a somatotopic manner by spontaneous muscle twitches<sup>8,9</sup>, motor patterns analogous to human fetal movements<sup>15,16</sup>. We suggest that the interaction between movement-triggered sensory feedback signals and self-organized spindle oscillations shapes the formation of cortical connections required for sensorimotor coordination.**

We examined the nature of early sensory signals and self-generated activity in the primary somatosensory (S1) cortex, using extracellular mapping and patch-clamp recordings in neonatal rats *in vivo* (postnatal days 1–8). In contrast to the adult neocortex<sup>17</sup>, activity in the neonatal rat was characterized by intermittent network bursts (mean±s.d. = 0.65±0.15 s), separated by long silent periods (Fig. 1; 7.2±1.93 s;  $n = 19$  non-anaesthetized pups). The multiple unit bursts were associated with a single sharp potential or spindle-shape field oscillations (10.8±1.2 Hz). Unitary discharges were rare between these field events (Fig. 1a, d). Sharp potentials occurred in isolation or preceded spindles by 100–200 ms. Simultaneous recording of field events in various S1 cortical layers with silicon probes showed a reversal of both the sharp potential and spindle pattern between superficial and deep layers (Fig. 1f;  $n = 2$  pups). Spindle activity was associated with rhythmic multiple unit discharges (Fig. 1b; see Supplementary Figures).

To explore the synaptic mechanisms underlying the generation of S1 network bursts, we employed patch-clamp recordings in urethane-anaesthetized animals (Fig. 2; see Supplementary Figures). Glutamatergic excitatory postsynaptic currents (EPSCs) and GABA ( $\gamma$ -aminobutyric acid) receptor A (GABA<sub>A</sub>) receptor-mediated PSCs were separated by using whole-cell recordings in voltage-clamp mode with low-chloride internal solution. The basic parameters of EPSCs and GABA<sub>A</sub>-PSCs were similar to that described *in vitro* (Supplementary Table)<sup>18</sup>. A characteristic feature of synaptic activity in S1 neurons was the grouping of both EPSCs

and GABA<sub>A</sub>-PSCs into bursts, which coincided with the S1 network events, recorded by a nearby extracellular electrode (Fig. 2b, c). Coincidence of synaptic and population activities was also reflected by the robust cross-correlations between the synaptic currents and S1 bursts and spindles (Fig. 2d, e). Charge transfer mediated by glutamatergic EPSCs and GABA<sub>A</sub>-PSCs during spindle bursts was  $32 \pm 7$  pC and  $71 \pm 29$  pC, respectively ( $n = 10$  cells). Thus, synchronous excitation of S1 neurons during spindle bursts is brought about by synaptic mechanisms involving glutamatergic connections and by GABAergic synapses in keeping with previous *in vitro* studies<sup>14,19,20</sup>.

On the basis of event duration, frequency, field waveform, cortical depth profiles and cellular correlates, S1 cortical spindles are homologous to sleep spindles or  $\mu$  rhythm of the adult cortex, suggesting the involvement of the thalamo-cortical network<sup>17,21–23</sup>. In support of this hypothesis, recordings from the thalamus ( $n = 4$  pups) revealed cortical spindle-related multiple unit discharges (see Supplementary Figures). However, besides being more variable in frequency, two features of S1 spindles were fundamentally different from the adult patterns: spindles in the pup were spatially highly confined and consistently associated with motor activity (Fig. 1). Motor patterns during the first week of life are characterized by spontaneous muscle twitches, limb jerks and whole-body startles<sup>8,9</sup>, initiated by stochastic bursts in the spinal cord network<sup>24</sup>. Video monitoring in freely moving pups ( $n = 4$ ) showed that most S1 bursts were associated with overt movement, including isolated muscle twitches, limb and whole-body jerks, crawling and sucking.

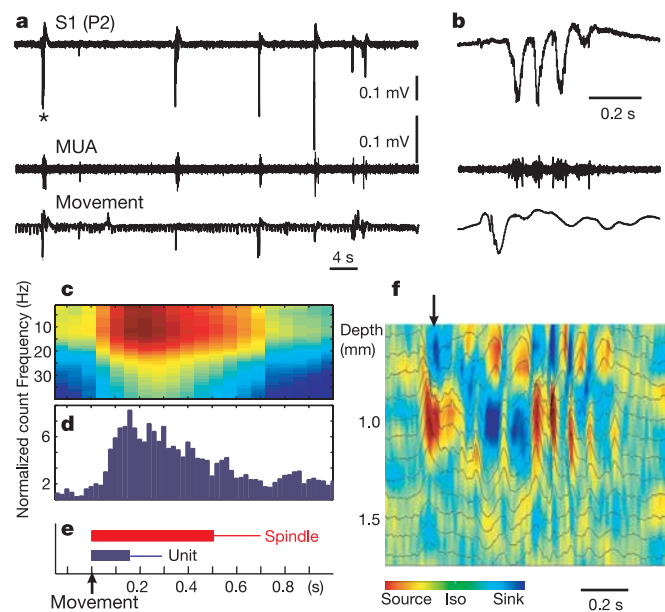


**Figure 1** Movement-triggered spindle bursts in S1 of the newborn rat. **a, b**, Wide-band recordings of extracellular activity and filtered (0.3–5 kHz) multiple unit activity (MUA) in S1 hindlimb area of a two-day-old (P2) behaving pup. Positivity is up. Bottom, movement of the contralateral hindlimb. Continuous rhythm reflects respiration. Note that field events and synchronized unit bursts are associated with movements. The event marked by an asterisk in **a** is shown at expanded time scale in **b**. **c, d**, Averaged power spectrogram of field (**c**) and perievent histogram of MUA (**d**), referenced to movement onset (0 s). Note increased power at 5–15 Hz (**c**, normalized colour code) and MUA rate (**d**, normalized spikes per bin) between 50 and 550 ms. The same pup was used in **a–d**. **e**, Mean ( $\pm$ s.d.) delay between movement peak and peak of spindle power, and movement and unit firing ( $n = 19$  pups;  $P < 0.001$  in each). **f**, Transcortical current source density of sharp potential (arrow) and spindle recorded by a 16-site silicone probe in a P5 pup. Colours indicate changes in current flow in (sink) and out (source) of neurons, relative to an isoelectric (iso) state.

Temporal analysis between mechanically detected movement and S1 activity showed that movement consistently preceded cortical unit bursts and associated sharp potentials and spindles (Fig. 1c–e). Only 14% ( $\pm 11$  s.d.) of all spindles occurred in the absence of overt movement. To investigate the spatial localization of S1 bursts, an array of eight electrodes was placed in the same cortical depth in 15 pups. Spindle bursts, associated with movements of the contralateral forelimb and hindlimb, were spatially confined to different cortical areas (Fig. 3a, b; see Supplementary Figures). After this step, the pups were lightly anaesthetized with urethane ( $1 \text{ g kg}^{-1}$ ) and the effect of sensory stimulation was examined. Mechanical touch ( $n = 15$ ) or electrical stimulation ( $n = 5$  additional pups) of the limbs and other body parts evoked a spatially confined sensory potential, often followed by a spindle. The magnitude, latency and cortical spatial distribution of the stimulation-evoked potential and spindle power were similar to that of sharp potentials and spindles triggered by the isolated, spontaneous limb movements (Fig. 3; see Supplementary Figures). The evoked field events were associated with multiple unit discharges and collective EPSCs and GABA<sub>A</sub>-PSCs (see Supplementary Figures). These results show that S1 spindle bursts are selectively triggered in a somatotopic manner by sensory feedback signals, resulting from spontaneous movements. Their spatial confinement, relative to adult sleep spindles<sup>17,21,22</sup>, may be explained by poorly developed long-range cortical connections at this early age<sup>3,25</sup>.

Is sensory input a necessary trigger for cortical spindles? To answer this question, sensory inputs from the hindlimb area were

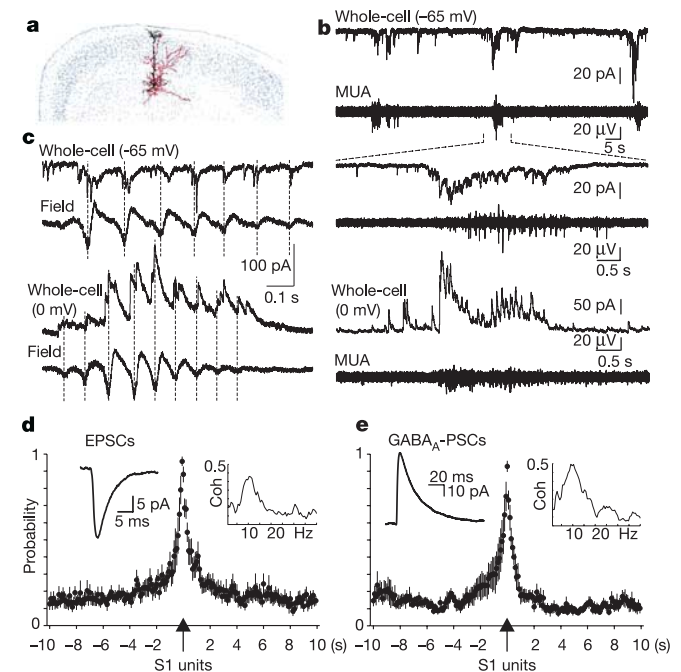


**Figure 2** Synaptic correlates of S1 spindle bursts. **a**, Reconstruction of a whole-cell recorded and biocytin-filled layer V pyramidal cell (red, axon; white, dendrites; depth,  $800 \mu\text{m}$ ; P5 pup). **b**, Voltage-clamp recording from the neuron in **a**, at holding potential  $-65 \text{ mV}$  (the reversal potential of the GABA<sub>A</sub>-receptor-mediated currents) and concomitant MUA (depth:  $900 \mu\text{m}$ ). The middle burst is shown at higher temporal resolution. Bottom traces, GABA<sub>A</sub>-PSCs at  $0 \text{ mV}$  (the reversal potential of the glutamatergic EPSCs) and concomitant MUA. **c**, Same as in **b** but from another cell (P6 pup). **d, e**, Normalized cross-correlograms between S1 MUA and EPSCs (**d**) and S1 MUA and GABA<sub>A</sub>-PSCs (**e**). Data represent the mean and s.e.m. from nine cells. Left insets, averaged spontaneous EPSCs and GABA<sub>A</sub>-PSCs from the neuron in **a** (see also Supplementary Table S1). Right insets, coherence (coh) spectra between field potential and PSCs for the neuron in **c**. Note high coherence at 10 Hz.

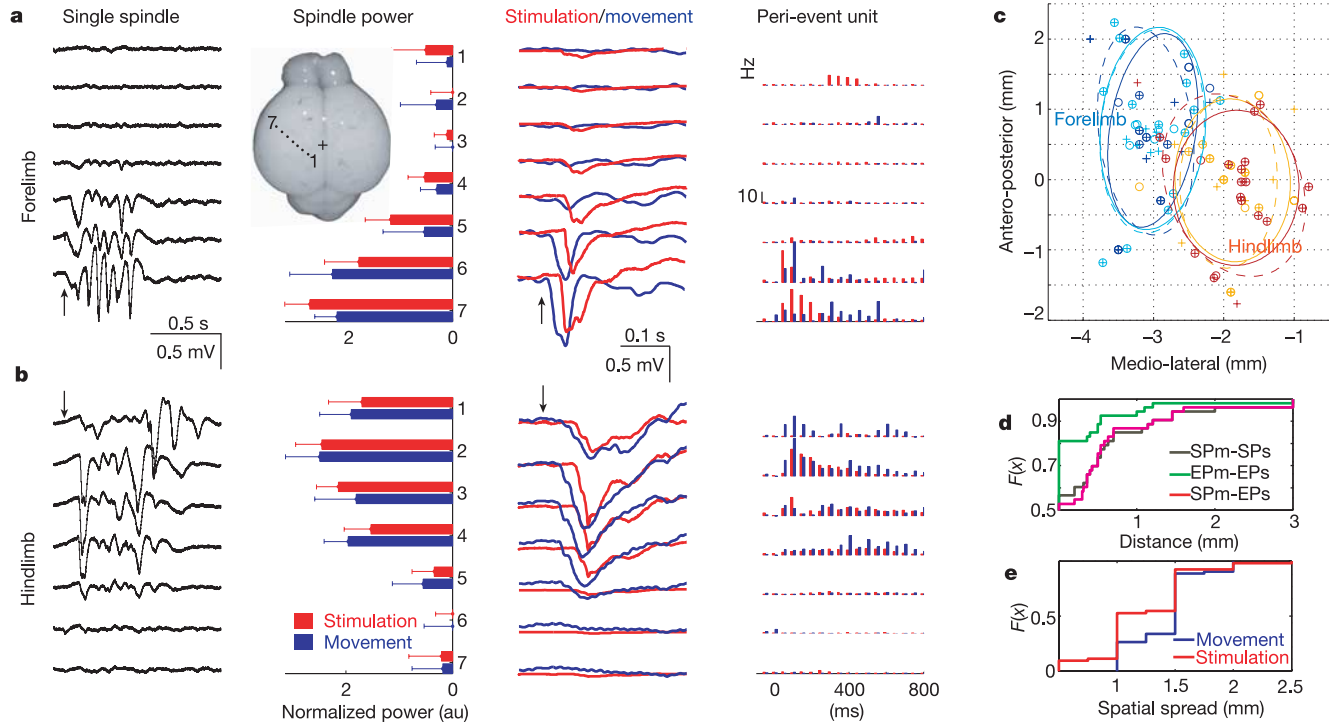


**Figure 3** Cortical spindles are spatially confined. **a**, First column: a single spindle event associated with contralateral forelimb jerk (arrow). Second column: power of spindle events triggered by spontaneous forelimb movement ( $n = 11$ , blue) or by touch stimulation of the forelimb ( $n = 34$ , red). Inset: position of recording electrodes. +, bregma. Third column: averaged field responses. Fourth column: peri-event time histograms of unit activity triggered by forelimb movement (blue) or touch stimulation (red). **b**, same as in **a**, but related to contralateral hindlimb activity ( $n = 20$  movements,  $n = 90$  stimulations). **c**, Spatial map (in stereotaxic coordinates) of maximal spindle

power (crosses) and amplitude of field potentials (circles), triggered by movement (blue, red) or evoked by touch (green, orange), referenced to forelimb (blue-green) and hindlimb (red-orange), based on 15 pups. Ellipsoids show 75% confidence intervals. **d**, Cumulative probability density function of distances between locations of maximal spindle power triggered by movement or touch stimulation (SPm-SPs), maximal amplitude of evoked potential by movement or touch (EPM-EPs), maximal spindle power by movement or evoked potential by touch (SPm-EPs). **e**, Cumulative probability density for effective spatial size of movement-triggered and touch stimulation evoked spindles.

disconnected by severing the spinal cord at low-thoracic level after mapping the topography of spontaneous and sensory evoked spindles ( $n = 5$  anaesthetized pups). The incidence of spindles in the hindlimb cortical area in the absence of peripheral input decreased threefold, but nevertheless spindles persisted. In the unaffected forelimb area spindle probability was not affected (Fig. 4). These findings provide evidence that spindles are self-organized patterns, generated by circuits that are intrinsic to the brain, but in the neonatal animal the movement-triggered events keep delaying the occurrence of spontaneous events because the rate of jerks is higher than that of the endogenous spindles.

In conclusion, the main pattern of activity in the newborn S1 cortex is a localized network burst, typically organized into a spindle pattern. Spindle bursts are consistently triggered in a somatotopic manner by sensory feedback from the characteristic neonatal muscle twitches, and limb and body jerks. Importantly, human fetal movements *in utero* are similar to the twitching movements in the neonatal rat<sup>8,15,16</sup> and, according to our findings, may be the main source of sensory inputs to the somatosensory cortex *in utero*. The scalp electroencephalogram (EEG) of preterm infants is characterized by intermittent bursts of electrical activity, often organized into rhythmic patterns (“delta-brush”)<sup>26</sup>, similar to the S1 spindles described here in the rat. Our experiments revealed a link between these two early developmental phenomena, S1 network spindles and spontaneous motor activity. Muscle activity in specific body parts is reliably and consistently associated with discharges of specific neuron groups in S1 cortex. The spatial-temporal coordination of movement (afferent feedback) spindle sequences may serve to anchor body representation in S1 cortex to the physical layout of

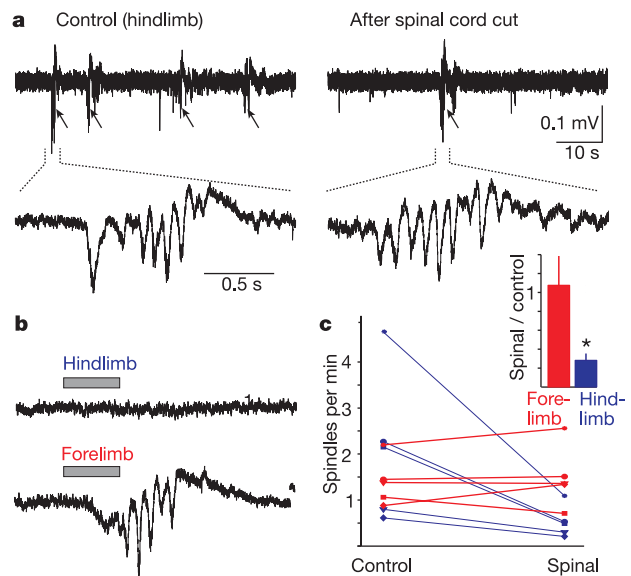


**Figure 4** Spindles can occur in the absence of sensory inputs. Effect of low-thoracic spinal cord transection on the neuronal activity in the hindlimb S1 area. **a**, Recordings from the hindlimb area before (left) and 90 min after (right) low-thoracic cut of the spinal cord. Arrows, spindle bursts. Two events are shown below at expanded time scale. **b**, Touch-evoked spindle events continued to occur after spinal transection in response to stimulation of the contralateral forelimb, but not hindlimb. **c**, Incidence of spindle events from five pups (P5–7) in the forelimb and hindlimb area before and after lesion. Bar graphs: mean (+s.d.) ratio of the frequency of spindle events before and after lesion ( $*P < 0.002$ ).

the muscular system and provide metric coordinates for sensation. As the initially slow-conducting thalamo-cortical and long-range motor-sensory connections develop<sup>3,25</sup>, the temporal prolongation of sensory feedback by the self-generated spindle may assist in strengthening the new connections, thus contributing to the establishment of sensorimotor coordination. □

**Methods**

Neocortical recordings were made from freely moving and anaesthetized neonatal rats (post-natal days (P) 1–8; *n* = 45)<sup>27</sup>. In freely moving pups (*n* = 7), 4–8 tungsten wires (20 μm in diameter) with 100–300 μm vertical tip separation were implanted at age P4 (–0.5–1.5 mm posterior to the bregma and 1.5–2.0 mm from the midline) under ice-cooling anaesthesia. In 17 additional pups (P1–P6), two anchor bars were fixed to the skull under isoflurane anaesthesia. After recovery, the head was restrained by the skull bars and the body was surrounded by a cotton nest, mimicking the presence of littermates<sup>28,29</sup>. An array of eight electrodes was placed in the same cortical depth in S1 so that at least some of them recorded units. A water heater placed under the nest kept the body temperature constant at 35 °C. Acute recordings (*n* = 21) were performed under urethane anaesthesia (1–1.5 g kg<sup>-1</sup>). For simultaneous recording of field potential and multi-unit activity, silicon probes<sup>30</sup> or tungsten wires (20 μm in diameter) were used. The silicon probe (16 recording sites with 100 μm separation) was inserted vertically into the brain so that simultaneous recordings could be made from the somato-sensory cortex at various depths. Whole-cell patch-clamp recordings were performed in the vicinity of the extracellular electrode (*n* = 9 rats)<sup>27</sup>. Morphological identification of the recorded cells was performed by adding biocytine (0.4%) to the pipette solution. Pyramidal cells with typical apical dendrite ramifying close to the brain surface were found in layer V (*n* = 4). Data were acquired at a sampling rate of 20 kHz and analysed off-line. Oscillatory events were detected by filtering the raw data in respective frequency ranges, identifying periods of high power of sufficient duration and then detecting the troughs. Multi-unit bursts were detected from the discriminated spike trains. Movements were recorded at 30 frames per second and reviewed frame-by-frame. The beginning and the end of all motor movements, including phasic and tonic, local and generalized movements were detected by eye. For finer temporal resolution, movements of the forelimb, hindlimb and body were detected by miniature earphones placed on the limbs. Sensitivity was sufficient to detect the smallest visible movements, including respiration-related displacement of the limbs (Fig. 1). Further details are provided in the Supplementary Methods.

Received 16 August; accepted 21 October 2004; doi:10.1038/nature03132.

1. Killackey, H. P., Rhoades, R. W. & Bennettclark, C. A. The formation of a cortical somatotopic map. *Trends Neurosci.* **18**, 402–407 (1995).
2. Armstrong-James, M. A. Spontaneous and evoked single unit activity in 7-day rat cerebral cortex. *J. Physiol. (Lond.)* **208**, 10P–11P (1970).
3. Lopez-Bendito, G. & Molnar, Z. Thalamocortical development: How are we going to get there? *Nature Rev. Neurosci.* **4**, 276–289 (2003).
4. Fox, K. A critical period for experience-dependent synaptic plasticity in rat barrel cortex. *J. Neurosci.* **12**, 1826–1838 (1992).
5. Fox, K. Anatomical pathways and molecular mechanisms for plasticity in the barrel cortex. *Neuroscience* **111**, 799–814 (2002).
6. Feldman, D. E., Nicoll, R. A. & Malenka, R. C. Synaptic plasticity at thalamocortical synapses in developing rat somatosensory cortex: LTP, LTD, and silent synapses. *J. Neurobiol.* **41**, 92–101 (1999).
7. Jain, N., Diener, P. S., Coq, J. O. & Kaas, J. H. Patterned activity via spinal dorsal quadrant inputs is necessary for the formation of organized somatosensory maps. *J. Neurosci.* **23**, 10321–10330 (2003).
8. Gramsbergen, A., Schwartz, P. & Precht, H. F. The postnatal development of behavioral states in the rat. *Dev. Psychobiol.* **3**, 267–280 (1970).
9. Petersson, P., Waldenstrom, A., Fahraeus, C. & Schouenborg, J. Spontaneous muscle twitches during sleep guide spinal self-organization. *Nature* **424**, 72–75 (2003).
10. Katz, L. C. & Shatz, C. J. Synaptic activity and the construction of cortical circuits. *Science* **274**, 1133–1138 (1996).
11. Katz, L. C. & Crowley, J. C. Development of cortical circuits: lessons from ocular dominance columns. *Nature Rev. Neurosci.* **3**, 34–42 (2002).
12. Yuste, R., Peinado, A. & Katz, L. C. Neuronal domains in developing neocortex. *Science* **257**, 665–669 (1992).
13. Yuste, R., Nelson, D. A., Rubin, W. W. & Katz, L. C. Neuronal domains in developing neocortex: mechanisms of coactivation. *Neuron* **14**, 7–17 (1995).
14. Garaschuk, O., Linn, J., Eilers, J. & Konnerth, A. Large-scale oscillatory calcium waves in the immature cortex. *Nature Neurosci.* **3**, 452–459 (2000).
15. de Vries, J. L., Visser, G. H. & Precht, H. F. The emergence of fetal behaviour. I. Qualitative aspects. *Early Hum. Dev.* **7**, 301–322 (1982).
16. Clancy, B., Darlington, R. B. & Finlay, B. L. Translating developmental time across mammalian species. *Neuroscience* **105**, 7–17 (2001).
17. Steriade, M. Impact of network activities on neuronal properties in corticothalamic systems. *J. Neurophysiol.* **86**, 1–39 (2001).
18. Kidd, F. L. & Isaac, J. T. Developmental and activity-dependent regulation of kainate receptors at thalamocortical synapses. *Nature* **400**, 569–573 (1999).
19. Ben Ari, Y. Developing networks play a similar melody. *Trends Neurosci.* **24**, 353–360 (2001).
20. Ben-Ari, Y., Khazipov, R., Leinekugel, X., Caillard, O. & Gaiarsa, J. L. GABA-A, NMDA and AMPA receptors: a developmentally regulated 'menage a trois'. *Trends Neurosci.* **20**, 523–529 (1997).
21. Steriade, M., McCormick, D. A. & Sejnowski, T. J. Thalamocortical oscillations in the sleeping and aroused brain. *Science* **262**, 679–685 (1993).
22. Destexhe, A. & Sejnowski, T. *Thalamocortical Assemblies: How Ion Channels, Single Neurons and Large-Scale Networks Organize Sleep Oscillations* (Oxford Univ. Press, New York, 2001).
23. Chatrian, G. E., Petersen, M. C. & Lazarte, J. A. The blocking of the rolandic wicket rhythm and some

- central changes related to movement. *Electroencephalogr. Clin. Neurophysiol.* **11** (Suppl.), 497–510 (1959).
24. O'Donovan, M. J. The origin of spontaneous activity in developing networks of the vertebrate nervous system. *Curr. Opin. Neurobiol.* **9**, 94–104 (1999).
25. Bureau, I., Shepherd, G. M. G. & Svoboda, K. Precise development of functional and anatomical columns in the neocortex. *Neuron* **42**, 789–801 (2004).
26. Dreyfus-Brisac, C. & Larroche, J. C. Discontinuous electroencephalograms in the premature newborn and at term. Electro-anatomo-clinical correlations [in French]. *Rev. Electroencephalogr. Neurophysiol. Clin.* **1**, 95–99 (1971).
27. Leinekugel, X. et al. Correlated bursts of activity in the neonatal hippocampus *in vivo*. *Science* **296**, 2049–2052 (2002).
28. Margrie, T. W., Brecht, M. & Sakmann, B. *In vivo*, low-resistance, whole-cell recordings from neurons in the anaesthetized and awake mammalian brain. *Pflügers Arch.* **444**, 491–498 (2002).
29. Karlsson, K. A. & Blumberg, M. S. Hippocampal theta in the newborn rat is revealed under conditions that promote REM sleep. *J. Neurosci.* **23**, 1114–1118 (2003).
30. Bragin, A. et al. Gamma (40–100 Hz) oscillation in the hippocampus of the behaving rat. *J. Neurosci.* **15**, 47–60 (1995).

Supplementary Information accompanies the paper on [www.nature.com/nature](http://www.nature.com/nature).

**Acknowledgements** We would like to thank T. Pankevych for helping with histological reconstruction, R. Cossart, D. Robbe, S. Montgomery and M. Zugaro for constructive comments. Supported by grants from the National Institutes of Health (G.B. and G.L.H.) and INSERM (R.K. and Y.B.-A.).

**Competing interests statement** The authors declare that they have no competing financial interests.

**Correspondence** and requests for materials should be addressed to G.B. (buzsaki@axon.rutgers.edu).

.....  
**A physical map of the chicken genome**

**John W. Wallis<sup>1</sup>, Jan Aerts<sup>2</sup>, Martien A. M. Groenen<sup>2</sup>, Richard P. M. A. Crooijmans<sup>2</sup>, Dan Layman<sup>1</sup>, Tina A. Graves<sup>1</sup>, Debra E. Scheer<sup>1</sup>, Colin Kremitzki<sup>1</sup>, Mary J. Fedele<sup>1</sup>, Nancy K. Mudd<sup>1</sup>, Marco Cardenas<sup>1</sup>, Jamey Higginbotham<sup>1</sup>, Jason Carter<sup>1</sup>, Rebecca McGrane<sup>1</sup>, Tony Gaige<sup>1</sup>, Kelly Mead<sup>1</sup>, Jason Walker<sup>1</sup>, Derek Albracht<sup>1</sup>, Jonathan Davito<sup>1</sup>, Shiao-Pyng Yang<sup>1</sup>, Shin Leong<sup>1</sup>, Asif Chinwalla<sup>1</sup>, Mandeep Sekhon<sup>1</sup>, Kristine Wylie<sup>1</sup>, Jerry Dodgson<sup>3</sup>, Michael N. Romanov<sup>3</sup>, Hans Cheng<sup>4</sup>, Pieter J. de Jong<sup>5</sup>, Kazutoyo Osoegawa<sup>5</sup>, Mikhail Nefedov<sup>5</sup>, Hongbin Zhang<sup>6</sup>, John D. McPherson<sup>7</sup>, Martin Krzywinski<sup>8</sup>, Jacquie Schein<sup>8</sup>, LaDeana Hillier<sup>1</sup>, Elaine R. Mardis<sup>1</sup>, Richard K. Wilson<sup>1</sup> & Wesley C. Warren<sup>1</sup>**

<sup>1</sup>Genome Sequencing Center, Washington University School of Medicine, Campus Box 8501, 4444 Forest Park Avenue, St Louis, Missouri 63108, USA  
<sup>2</sup>Animal Breeding and Genetics Group, Wageningen University, Marijkeweg 40, 6709 PG Wageningen, The Netherlands  
<sup>3</sup>Department of Microbiology and Molecular Genetics, Michigan State University, East Lansing, Michigan 48824, USA  
<sup>4</sup>Avian Disease and Oncology Laboratory, Agricultural Research Service, USDA, East Lansing, Michigan 48823, USA  
<sup>5</sup>Children's Hospital Oakland Research Institute, 5700 Martin Luther King Jr Way, Oakland, California 94609, USA  
<sup>6</sup>Department of Soil and Crop Sciences and Institute for Plant Genomics and Biotechnology, Texas A&M University, College Station, Texas 77843, USA  
<sup>7</sup>Department of Molecular and Human Genetics, Baylor College of Medicine, One Baylor Plaza Houston, Texas 77030, USA  
<sup>8</sup>Genome Sciences Centre, British Columbia Cancer Agency, 570 West 7th Avenue, Vancouver, British Columbia, V5Z 4E6, Canada

.....  
**Strategies for assembling large, complex genomes have evolved to include a combination of whole-genome shotgun sequencing and hierarchal map-assisted sequencing<sup>1,2</sup>. Whole-genome maps of all types can aid genome assemblies, generally starting with low-resolution cytogenetic maps and ending with the highest**